

Supporting Information for
Sunlight-Driven Chlorate Formation During Produce Irrigation with Chlorine- or
Chloramine-Disinfected Water

Min-Jeong Suh¹ and William A. Mitch^{1, *}

¹ Department of Civil and Environmental Engineering, Stanford University, 473 Via Ortega,
Stanford, California 94305, United States

*Contact Information: email: wamitch@stanford.edu, Phone: 650-725-9298, Fax: 650-723-7058

9 pages

8 figures

1 table

Contents

Figure S1: Chlorate levels in sequential rinsates from spinach coupons	S3
Figure S2: Effect of phosphate buffer on initial chlorate concentrations	S3
Figure S3: Chlorate formation in chlorine under natural solar irradiation	S4
Text S1: Radical reactions with free chlorine leading to chlorate formation	S4
Figure S4: Absorbance spectra of HOCl, OCl ⁻ and monochloramine	S5
Figure S5: Chlorate formation from chlorine under various light conditions in the solar simulator	S5
Text S2: Comparison of observed and predicted chlorate concentrations in Figure 1C	S6
Figure S6: Plot of observed against predicted chlorate concentration	S6
Figure S7: Chlorate formation at 21 and 27 °C in the solar chamber	S7
Figure S8: Percentage chlorate recovery in rinsate and inside vegetable in various plants	S7
Table S1: Summary of the statistical analysis on the average chlorate levels in the vegetables treated with different irradiation conditions and disinfectants	S8

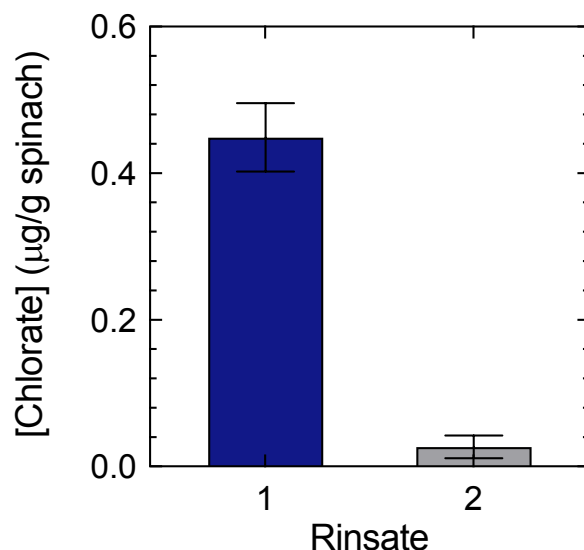


Figure S1: Chlorate concentrations in rinsates from sequential rinses from 2 cm × 2 cm spinach coupons after application of 0.25 mL of 1 mg/L chlorate solution droplets. The spinach coupons were treated for 6 h, a time sufficient for complete evaporation of the droplets. After the experiment, each spinach coupon was rinsed with 1 mL deionized water (rinsate 1). Each rinsed spinach coupon was rinsed with another 1 mL deionized water (rinsate 2). Error bars represent the standard error of experimental triplicates.

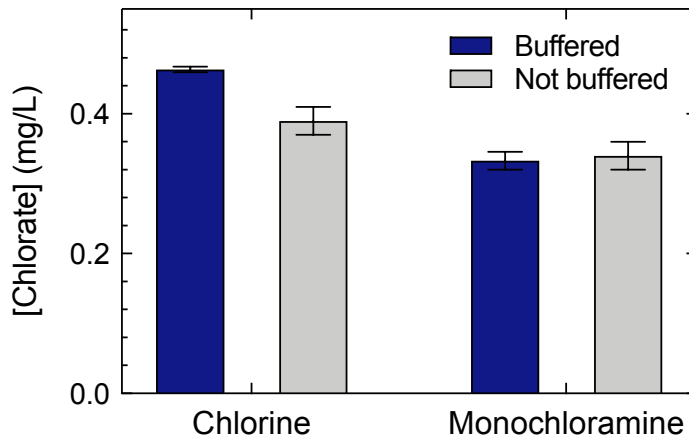


Figure S2: Effect of phosphate buffer on the initial chlorate concentrations in 50 μM chlorine and monochloramine solutions at 21 °C. Unbuffered chlorine and monochloramine solutions were at pH values of 10.5 and 9.4, respectively. Buffered solutions were prepared at pH 7 using 2.5 mM phosphate buffer.

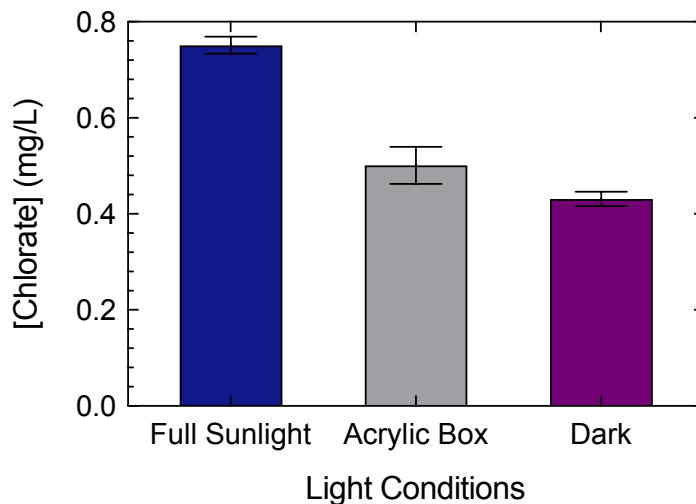
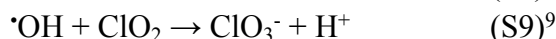
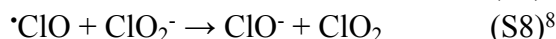
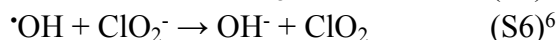
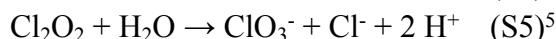
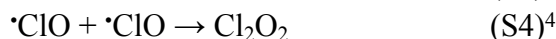
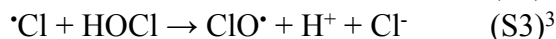
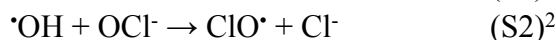


Figure S3: Chlorate concentrations in 50 μM (3.6 mg/L as Cl_2) chlorine solutions in deionized water at pH 7 (2.5 mM phosphate buffer) after 71 min of natural solar irradiation. Experiments were conducted in April (2020) near noon in Menlo Park, CA over two successive days. The average results are plotted. The average total incident photon flux was measured to 0.33 kW m^{-2} between 280-700 nm and 0.074 kW m^{-2} between 280-400 nm. The fluence over 71 min of irradiation was 1067 and 1753 kJ m^{-2} between 280-700 nm on the first and second day, respectively. The average temperatures during the experiment were 33 and 30 $^{\circ}\text{C}$ for the first and second day, respectively. Error bars represent standard errors from experimental replicates ($n = 6$ for full sunlight and dark samples; $n = 4$ for samples under the acrylic box).

Text S1: Radical reactions with free chlorine leading to chlorate



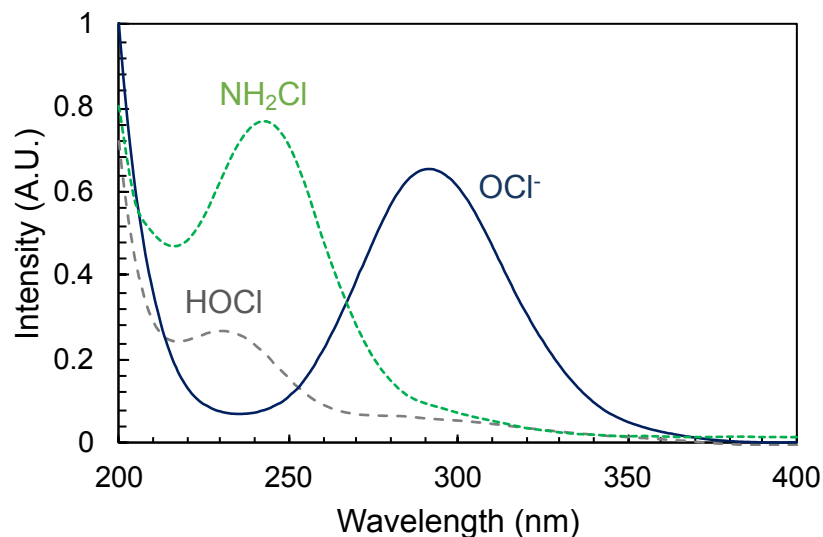


Figure S4: Absorbance spectra of chlorine (1.7 mM) solution at pH 5.5 (HOCl) and pH 9 (OCl⁻), and monochloramine stock solution (1.7 mM).

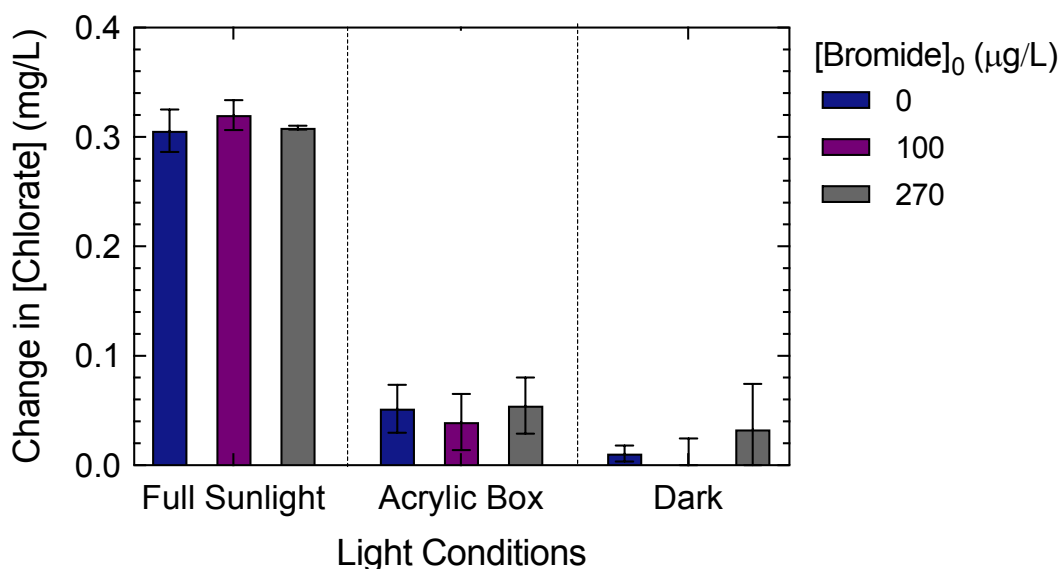


Figure S5: Change in chlorate concentrations in 50 μM chlorine solutions after 180 min treatment under various light conditions (full sunlight, under acrylic box, and dark) in a solar simulator at 21 °C at various pH buffered with 2.5 mM phosphate. The fluence absorbed by the solution were 1258 and 54 kJ m⁻² under full sunlight condition and under the acrylic box, respectively, for 280-700 nm. The acrylic box was used to shield wavelengths < 370 nm. Error bars represent the standard error of experimental triplicates.

Text S2: Comparison of observed and predicted chlorate concentrations in Figure 1A.

The chlorate concentrations measured in Figure 1A were predicted using equation S10, where $[\text{ClO}_3^-]_0$ is the initial chlorate concentration (0.49 mg/L), $\text{MY}_{\text{ClO}_3^-}$ is the 7.2 molar yield of chlorate relative to chlorine degraded, and k_{obs} is the predicted first order observed degradation rate of OCl^- from equation 7, where $\phi_{\text{obs},\text{OCl}^-}$ is the 0.72 observed quantum yield for OCl^- photodegradation.

$$[\text{ClO}_3^-] = [\text{ClO}_3^-]_0 + \text{MY}_{\text{ClO}_3^-} [\text{OCl}^-]_0 (1 - e^{-k_{\text{obs}}t}) \quad (\text{S10})$$

$$k_{\text{obs}} = 2.303 \phi_{\text{obs},\text{OCl}^-} I \sum_{280}^{380} (I\epsilon) \quad (\text{S11})$$

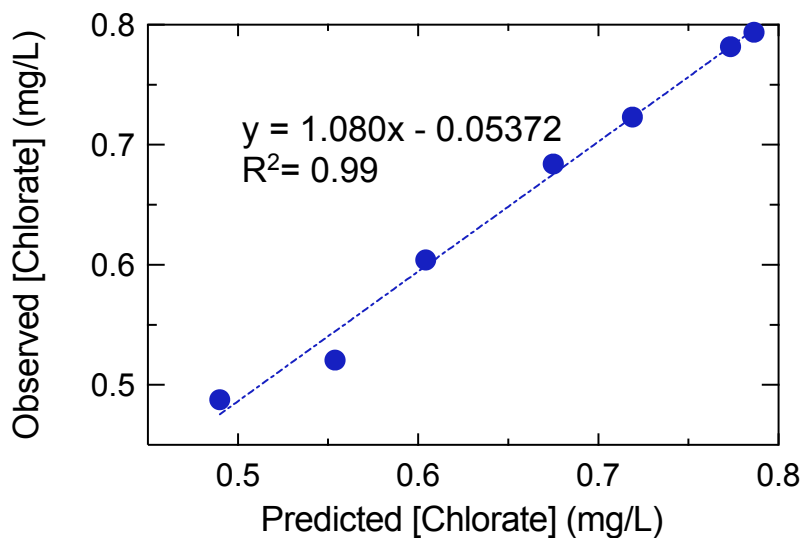


Figure S6: Plot of average chlorate concentration measured in the experiment for Figure 1A against chlorate concentration predicted by equation S10. Chlorate formation was measured during treatment of 50 μM (3.6 mg/L as Cl_2) chlorine solution in a solar simulator (photon flux of 0.12 kW m^{-2} between 280-700 nm) at 21 $^\circ\text{C}$ and pH 7 (2.5 mM phosphate buffer) at time points $t = 0, 10, 20, 40, 60, 120$ and 180 min.

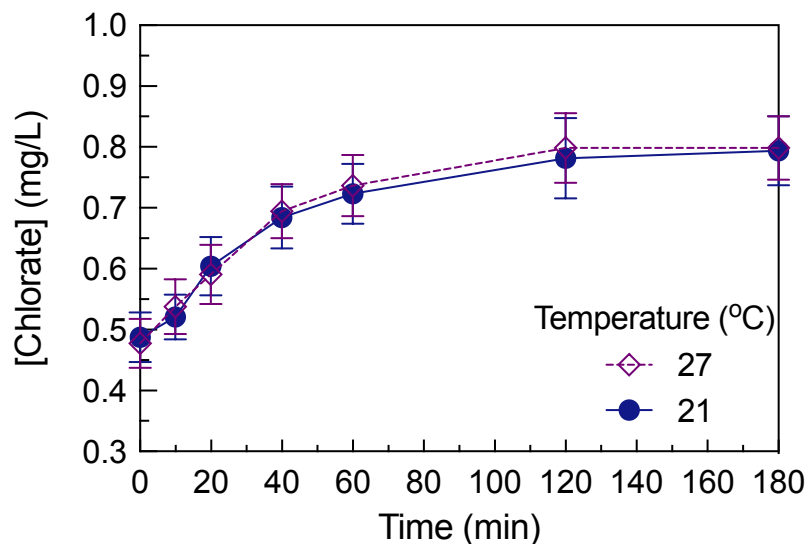


Figure S7: Chlorate formation during treatment of 50 μM (3.6 mg/L as Cl_2) chlorine solutions in a solar simulator at 21 and 27 $^{\circ}\text{C}$ and pH 7 (2.5 mM phosphate buffer). The reaction temperature was controlled using a water bath. All other experimental conditions (i.e., photoreactor light intensity setting, experimental methods) were the same as the experimental conditions for **Figure 1A**. Error bars represent the standard error of experimental triplicates.

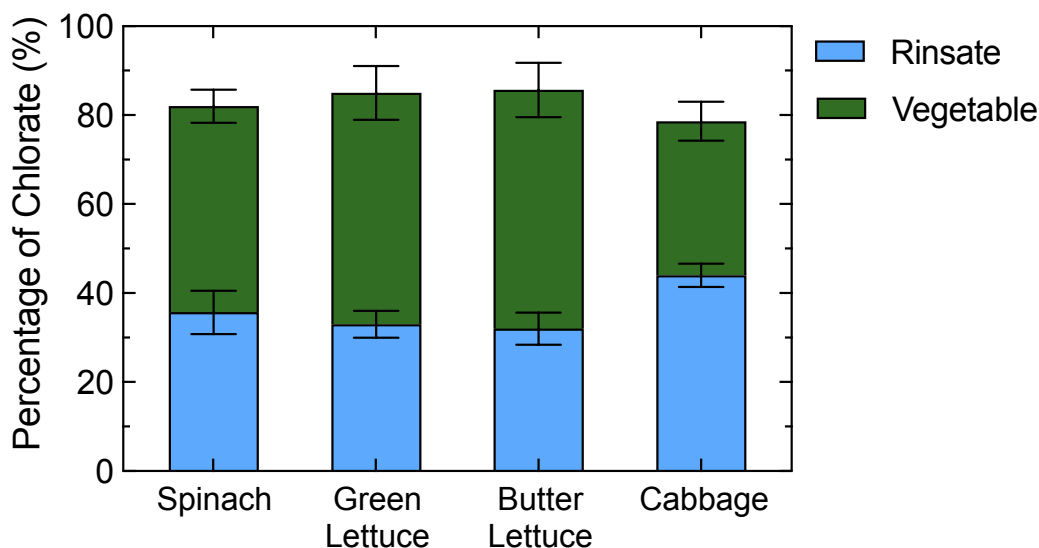


Figure S8: Percentages of chlorate recovered from spinach, green lettuce, butter lettuce and cabbage in the rinsate and inside the vegetable, respectively. All vegetables were bought from Whole Foods Market. After thoroughly rinsing the leaves in deionized water, excess water was removed using a salad spinner and Kim wipes. Each leaf surface experiment was conducted using ~ 0.8 g leaves placed in a petri dish. The wet leaf mass used for each experiment was individually recorded and used to calculate chlorate yields on a μg chlorate/g wet weight basis. One mL of 3 mg/L chlorate solution was deposited on each leaf. Each sample was treated for 16 h, a time sufficient to evaporate droplets from all vegetables except cabbage, at 7 $^{\circ}\text{C}$ to minimize

deterioration of the plant material. Since the solution droplets on cabbage leaves had not fully evaporated, the chlorate level in the rinsate may be less accurate than those in rinsates from other vegetables. The vegetable samples were processed using the experimental procedure for chlorate analysis of spinach coupons.

Table S1: Summary of the statistical analysis to test the effect of irradiation and disinfectant type on average chlorate levels in chicory, cabbage, lettuce and spinach.

	ANOVA Statistics			
	Chicory	Cabbage	Lettuce	Spinach
Irradiation	F(1, 32)= 37.7; p < 0.05	F(1, 32)= 10.6; p < 0.05	F(1, 32)= 16.2; p < 0.05	F(1, 8)= 5.64; p < 0.05
Disinfectant Type	F(1, 32)= 117; p < 0.05	F(1, 32)= 5.2; p < 0.05	F(1, 32)= 60.3; p < 0.05	F(1, 8)= 21.7; p < 0.05

The degrees of freedom for the between-groups and residual associated with the calculated F-test result and the resulting probability value.

References:

- (1) Matthew, B. M.; Anastasio, C. A Chemical Probe Technique for the Determination of Reactive Halogen Species in Aqueous Solution: Part 1 - Bromide Solutions. *Atmospheric Chemistry and Physics* **2006**, 6 (9), 2423–2437.
- (2) Connick, R. E. The Interaction of Hydrogen Peroxide and Hypochlorous Acid in Acidic Solutions Containing Chloride Ion. *J. Am. Chem. Soc.* **2002**, 69 (6), 1509–1514.
- (3) Zehavi, D.; Rabani, J. The Oxidation of Aqueous Bromide Ions by Hydroxyl Radicals. A Pulse Radiolytic Investigation. *J. Phys. Chem.* **1972**, 76, 3, 312-319.
- (4) Sun, P.; Lee, W.-N.; Zhang, R.; Huang, C.-H. Degradation of DEET and Caffeine under UV/Chlorine and Simulated Sunlight/Chlorine Conditions. *Environ. Sci. Technol.* **2016**, 50, 24, 13265-13273.
- (5) Kormányos, B.; Nagypál, I.; Peintler, G.; Horváth, A. K. Effect of Chloride Ion on the Kinetics and Mechanism of the Reaction between Chlorite Ion and Hypochlorous Acid. *Inorg. Chem.* **2008**, 47, 17, 7914-7920.
- (6) Eriksen, T. E.; Lind, J.; Merényi, G. Generation of Chlorine Dioxide from ClO by Pulse Radiolysis. *J. Chem. Soc., Faraday Trans. 1* **1981**, 77 (9), 2115–2123.
- (7) Chuang, Y. H.; Chen, S.; Chinn, C. J.; Mitch, W. A. Comparing the UV/Monochloramine and UV/Free Chlorine Advanced Oxidation Processes (AOPs) to the UV/Hydrogen Peroxide AOP under Scenarios Relevant to Potable Reuse. *Environ. Sci. Technol.* **2017**, 51, 23, 13859–13868.
- (8) Alfassi, Z. B.; Huie, R. E.; Mosseri, S.; Neta, P. Kinetics of One-Electron Oxidation by the ClO Radical. *Int. J. Radiat. Appl. Instrum. Part C.* **1988**, 32 (1), 85–88.
- (9) K. Klaning, U.; Sehested, K.; Holcman, J. Standard Gibbs Energy of Formation of the Hydroxyl Radical in Aqueous Solution. Rate Constants for the Reaction Chlorite (ClO_2^-) + Ozone \leftrightarrow Ozone(1-) + Chlorine Dioxide. *J. Phys. Chem.* **2002**, 89 (5), 760–763.